HHS Public Access

Author manuscript

Biomaterials. Author manuscript; available in PMC 2019 September 01.

Published in final edited form as:

Biomaterials. 2018 September ; 178: 363–372. doi:10.1016/j.biomaterials.2018.05.007.

Recyclable Magnetic Nanoparticles Grafted with Antimicrobial Metallopolymer-Antibiotic Bioconjugates

Parasmani Pageni[†], **Peng Yang**[†], **Marpe Bam**[‡], **Tianyu Zhu**[‡], **Yung Pin Chen**[§], **Alan W. Decho**[§], **Mitzi Nagarkatti**[‡], and **Chuanbing Tang**[†,*]

[†]Department of Chemistry and Biochemistry, University of South Carolina, Columbia, South Carolina 29208, United States

[§]Department of Environmental Health Sciences, University of South Carolina, Columbia, South Carolina 29208, United States

[‡]Department of Pathology, Microbiology and Immunology, University of South Carolina, School of Medicine, Columbia, South Carolina 29209, United States

Abstract

Over-prescription and improper use of antibiotics has led to the emergence of bacterial resistance and now poses a major threat to public health. There has been significant interest in the development of alternative therapies and agents to combat antibiotic resistance. We report the preparation of recyclable magnetic iron oxide nanoparticles grafted with charged cobaltocenium-containing metallopolymers by surface-initiated reversible addition-fragmentation chain transfer (RAFT) polymerization. β-Lactam antibiotics were then conjugated with metallopolymers to enhance their vitality against both Gram-positive and Gram-negative bacteria. The enhanced antibacterial activity was a result of synergy of antimicrobial segments that facilitate the inhibition of hydrolysis of antibiotics and local enhancement of antibiotic concentration on a nanoparticle surface. These magnetic nanoparticles can be recycled numerous times without losing the initial antimicrobial potency. Studies suggested negligible toxicity of metallopolymer-grafted nanoparticles to red blood cells and minimal tendency to induce resistance in bacteria.

Keywords

Antimicrobial resistance; Metallopolymers; Magnetic nanoparticles; Cationic polyelectrolytes; Metallocene

[*]Corresponding Author: tang4@mailbox.sc.edu.

Notes: The authors declare no competing financial interest.

Appendix A. Supplementary data: Supplementary data related to this article can be found at https://doi.org/10.1016/

Introduction

The emergence of antibiotic resistance is not only a threat to global health but also to the economy. Antibiotic resistance infections result in increased mortality and excess costs in both clinical and community settings. According to a report by CDC, it is now predicted that global mortality by bacterial infection would reach 10 million annually by the year 2050 and cost an estimated $100 trillion dollars in lost economic output[1]. As a result of excessive use, traditional antibiotics exhibit a rapidly decreased efficacy. In some cases, infections become untreatable and more patients succumb from other conditions such as AIDS, whose etiology is complicated by antibiotic resistance infections[2]. This threatens many of the most significant medical advances that have been made, and results in increasing therapeutic costs and extended hospitalization. The antibiotics have lost their efficacy gradually as a result of emergence and circulation of antibiotic resistance among bacteria. Inspired by antimicrobial peptides, synthetic polymers containing cationic groups like quaternary ammonium or sulfonium have been studied extensively and almost exclusively as a measure to fight back bacterial resistance due to the physical nature of their action of damage to the membranes[3-11]. However, the less selective mode of action of these polymers results in toxicity towards mammalian cells, and thus the quest persists for safer, more-effective antimicrobial agents.

Nanomaterials have been gaining much attention as antimicrobials that are complementary to antibiotics, and fill important gaps where antibiotics often fail[12]. The diversity of nanoparticles that are currently in use ranges from metal, metal oxides to organic forms. Nanoparticles can be engineered with high specificity to produce surfaces having different types of functional groups, charges and other properties. Magnetic nanoparticles have been an area of interest for researchers from a wide range of disciplines including catalysis[13, 14], data storage[15, 16], environmental remediation[17], magnetic resonance imaging[18] and biomedicines[19-22]. In particular, a wide variety of biomedical applications range from contrast agents for magnetic resonance imaging to the deterioration of cancer cells via hyperthermic treatment[23].

Specifically, iron oxide particles, with size ranges of nanometer scale, display superparamagnetic properties and could interact magnetically with each other when not properly stabilized. Due to their extremely large surface-to-volume ratio and the large surface energy, magnetic nanoparticles tend to aggregate. In addition, naked metallic nanoparticles have a high chemical activity and are prone to oxidation in air resulting in loss of magnetism and dispersibility[24]. To circumvent these problems, it is essential to protect and stabilize the naked magnetic nanoparticles by using either ionic compounds or large molecules such as polymers or surfactants containing long hydrocarbon chains. Polymer grafting has become a popular technique for tuning the surface properties of nanoparticles[25-29]. Also, magnetic nanoparticles without polymer coatings often aggregate in water or tissue fluid, which may limit their applications. Grafting of polymers not only stabilizes the nanoparticles but also opens the door for further functionalization.

Antibiotics have been the major therapy to treat various kinds of bacterial infections for nearly a century. However, there is hardly any class of antibiotics that has escaped the

resistance mechanism by bacteria. The time interval between the launch of a new antibiotic in clinical practice and the emergence of resistance has been variable and rapidly shortening over the past century[30]. The strategy of discovering and developing new antibiotics is necessary but may not address the concern of bacterial resistance for long. The approach to breathe life into traditional antibiotics and antimicrobial agents using new therapeutic approaches to treat infection-associated diseases seems fruitful and addresses the urgent need and provides economic incentives.

We postulated that linking antimicrobial agents to nanoparticles may represent a powerful, yet adaptable tool to more-efficiently limit antibiotic-resistant infections. We recently developed a class of charged cobaltocenium-containing metallopolymers with minimal toxicity and good antimicrobial efficacy[31-33]. These metallopolymers not only kill the bacteria but also protect β-lactam antibiotics from the detrimental hydrolysis of β-lactamase enzyme.

Herein we report new work on grafting cobaltocenium-containing polymers from iron oxide nanoparticles using surface-initiated reversible addition-fragmentation chain transfer (SI-RAFT) polymerization (Scheme 1). In doing so, the magnetic properties of nanoparticles compliment the antimicrobial features of cobaltocenium-containing polymers, and result in a new class of materials having highly-applicable characteristics such as magnetic antimicrobial nanoparticles that can impact therapies to tackle rampant bacterial infections. These nanoparticles were then conjugated with β-lactam antibiotics, such as penicillin, *via* ion-pairing between the cationic cobaltocenium moiety in the nanoparticles and the carboxylate anion of antibiotics. The newly-synthesized nanoparticle conjugates displayed significantly enhanced antimicrobial efficacy against both Gram-positive and Gram-negative strains. In addition, they can be recycled for at least 15 passages without losing the potency.

Results and Discussion

1. Synthesis of Cobaltocenium-Containing Iron Oxide Nanoparticles

We introduced cationic cobaltocenium along with antibiotics onto iron oxide nanoparticles to form magnetic antimicrobial nanoparticles, as shown in Scheme 1. To be specific, cobaltocenium-containing polymers were grafted from iron oxide nanoparticles, which were then installed with penicillin via ionic complexation. Cobaltocenium, a cationic and high-oxidation state metallocene, has recently gathered a lot of attention for its various applications derived from its excellent chemical stability and superior binding ability to anions[34-42]. The pathway for the synthesis of magnetic nanoparticles consisted of the formation of iron oxide nanoparticles by coprecipitation of Fe^{2+} and Fe^{3+} salts in the presence of an alkaline solution followed by the immobilization of RAFT agent on to the nanoparticle surface. The commonly-used coprecipitation method was chosen because of its simplicity, low cost and high efficiency [43]. The surface of nanoparticles was further functionalized with 3-aminopropyldimethylethoxysilane followed by an amidation reaction between its amino group and acid group of an RAFT agent, 4-cyanopentanoic acid dithiobenzoate (CPDB)[44]. The amount of RAFT agent anchored onto the modified iron oxide nanoparticles was quantitatively determined by comparing the absorption for CPDB

from iron oxide nanoparticles to free CPDB. The grafting density was found to be 0.15 chain/nm^2 (16.5 μmol/g CPDB).

In conjunction with well-developed controlled radical polymerization techniques, especially RAFT, the “grafting from” strategy provides an efficient route to functionalize surface by controlling compositions and structures[45-49]. RAFT polymerization provides quantitative and precise control over the molecular weight[50, 51]. The next step was mediated by CPDB-coated iron oxide nanoparticles to carry out polymerization of a monomer, 2-cobaltocenium amidoethyl methacrylate hexaflurophosphate (CoAEMAPF$_6$), using AIBN as an initiator in dry DMF at 90 °C, as shown in Scheme 2. CoAEMAPF$_6$ was synthesized using a previously established procedure[52]. Cobaltocenium-containing polyelectrolytes with hydrophobic anions can be easily switched to hydrophilic ones using tetra-butylammonium salts via a facile phase-transfer ion-exchange method[53]. In this case, the nanoparticles with PF_{6-} anions were subjected to ion exchange, which resulted in hydrophilic chloride-paired nanoparticles. The newly formed nanoparticles had good aqueous solubility, which opened the door for use in biomedicines. The nanoparticles were further conjugated with anionic penicillin-G (i.e. penicillin, hereafter) via electrostatic interaction between the cationic cobaltocenium moiety and anionic penicillin by mixing them together. Any unbound penicillin was removed by dialysis.

The mean diameter of cobaltocenium-containing nanoparticles was ~ 25 nm as measured by dynamic light scattering and was consistent with measurements obtained by TEM, as shown in Figure 1. After loading penicillin to the nanoparticle by electrostatic interaction, the diameter rose up to 33 nm as seen in DLS. The nanoparticle was also characterized by FTIR and EDX elemental analysis to confirm major chemical bonds and elements in the nanoparticles, respectively (Figures S1 and S2). Thermogravimetric analysis (TGA) was implemented to determine the accurate weight loss of nanoparticles after loss of attached organic compounds. The TGA of iron oxide nanoparticles with RAFT agent and cleaved polymer chains was compared with that of cobaltocenium-containing iron oxide nanoparticles alone (Figure S3). Based on the TGA measurement, the total weight percentage of cobaltocenium in the iron oxide nanoparticle (FeNP) was 56 wt%. It was found that cationic cobaltocenium moiety complexed with carboxylate anions of penicillin at a 1:1 pairing. This allowed us to calculate the final weight percentage of penicillin in the nanoparticles to be around 30 wt%.

2. Antimicrobial Activity of Cobaltocenium-Containing Iron Oxide Nanoparticles

The nanoparticles were tested for their antimicrobial activity against two different Gram-positive, *Staphylococcus aureus* (ATCC 33591) and *Bacillus cereus* (ATCC 11778), and three different Gram-negative bacteria, *Escherichia coli* (ATCC 11775), *Proteus vulgaris* (ATCC 33420) and *Klebsiella pneumonia* (ATCC 35596), by the conventional agar disk-diffusion assay following a protocol of Kirby Bauer diffusion test[54]. Initially, concentrations of penicillin ranging from 4 μg to 10 μg were tested. The optimal antibacterial activity was obtained with 7 μg penicillin and was used for all subsequent disk diffusion assays. The development of a clear zone around the disk represents an inhibition zone, which indicates the ability of the test samples to kill the bacteria. To better compare

the antimicrobial efficacy, four different samples were prepared for disk diffusion assays: homopolymer-penicillin conjugate (PCo-Pen), penicillin, FeNP-penicillin conjugate (FeNP-Pen) and FeNP without penicillin (FeNP-Cl). For *S. aureus,* the diameter of the inhibition zone caused by penicillin alone was 8 mm while the homopolymer conjugate resulted in a larger diameter of 11 mm, as shown in Figure 2 and Figure S4. When the FeNP-penicillin conjugate was used, the inhibition zone was significantly enhanced and diameters increased to a mean of 18 mm. FeNP nanoparticles lacking penicillin had much smaller zones of inhibition owing to their much reduced antibacterial activity. When the assay was extended to another Gram-positive bacterium, *B. cereus*, a similar trend was observed, however, higher antimicrobial activities for all samples were observed. The zones of inhibition of penicillin and FeNP-penicillin conjugates increased to 10 mm and 20 mm, respectively, when compared to *S. aureus*. For further investigation, disk diffusion assays were carried out against several BSL2-level Gram-negative pathogen strains using the above-mentioned protocol: *Escherichia coli, Proteus vulgaris* and *Klebsiella pneumonia.* As shown in Figure 2, penicillin alone showed minimal antibacterial activity when compared to homopolymer-penicillin conjugates and FeNP-penicillin conjugates. For example, inhibition zones caused by penicillin were just 4 mm against *K. pneumonia,* while inhibition zones created by FeNP-penicillin conjugate were three times higher (12 mm). Inhibition zones caused by homopolymer conjugate (PCo-Pen) were larger than those of penicillin alone, but remainded smaller than the FeNP-penicillin conjugates. The cationic moiety of cobaltocenium displayed good antimicrobial activity at a higher concentration, but the concentration of cobaltocenium in the FeNP-Cl was probably not high enough to result in determinable antimicrobial activity. Compared to penicillin alone, all FeNP-conjugates exhibited much stronger antimicrobial activities for both Gram-positive and Gram-negative strains.

For penicillin and each of the FeNP-penicillin conjugates, minimum inhibitory concentrations (MIC) were calculated using the established protocol, and are given in Table 1[55]. The MIC values are based on the effective concentration of penicillin in the nanoparticle-penicillin conjugate. The mean MIC of FeNP-penicillin conjugates against Gram-positive strains, *S. aureus* was 3.4±0.4 μg/mL and *B. cereus* was 2.7 ±0.5 μg/mL, which was approximately four times lower than that of penicillin alone, 13.48 μg/mL and 10.92 μg/mL respectively, for these pathogens.

As expected, the MIC values for three different Gram-negative strains were significantly higher. They followed a similar trend to the Gram-positive strains, and have much lower MIC values than those observed for penicillin alone. Compared with penicillin, nanoparticle-polymer conjugates produced significantly higher efficacies against both Gram-positive and Gram-negative strains. The additional outer polysaccharide layer (i.e. capsule) present in the Gram-negative bacteria might act as an extra layer of shielding for the test samples to penetrate, resulting in the observed smaller inhibition zones and higher MIC values.

The increased bactericidal activity and inhibition effect of FeNP-penicillin conjugates on various Gram-positive and Gram-negative strains was further confirmed by confocal scanning laser microscopy (CSLM) and scanning electron microscopy (SEM). LIVE/DEAD stained bacteria viability assays using CSLM indicated greater levels of cell death and lower

cell densities when bacterial cells were exposed to FeNP-Pen conjugates, as shown in Figure 3. Cells incubated with FeNP-Pen conjugates displayed primarily red or yellow fluorescence, indicative of cell death, as determined by rupture of cell membranes. The decrease in the number of bacteria is possibly due to the bactericidal action. Also, the SEM imaging was used to compare differences in morphology before- and after-treatment with FeNP-Pen conjugates (Figure 4). Control samples consisted of intact bacterial cells with smooth surfaces while the cells incubated with nanoparticle conjugates displayed collapsed cell envelopes with obvious disruptions in the original morphology.

We postulated that the high antibacterial efficacy resulted from the stable attachment of polymers to the nanoparticle surface, which in turn delivered increased concentrations of antibacterial species to the target bacterial cells. The bacterial cell wall is the primary target of β-lactam antibiotics such as penicillin, and bacteria usually resist these antibiotics by secreting beta-lactamase enzymes, which cause the hydrolysis of the lactam ring and nullify the efficacy of antibiotic molecules. The synergistic introduction of two antimicrobial species, cobaltocenium and penicillin, acts through different mechanisms against the pathogenic bacteria. Thus, the possibility of circumventing both mechanisms by bacteria, in addition to the local concentration effect provided by nanoparticles, is significantly reduced, leading to enhanced antibacterial activity. When antibiotics are administered in a solution form, the concentration of antibiotic reaching the pathogenic cell is much reduced as the resulting scenario is much different as they tend to form a homogenous dispersion of molecules spread over the tissues.

One of the advantages using iron oxide nanoparticles is that the FeNP-penicillin conjugates can be easily extracted and recycled owing to the fast response to an applied magnetic field as shown in Scheme 3. This not only saves the cost and time but also eliminates the possibility of nano-pollution in the biological environment. The dynamic shake flask method was used to evaluate the recyclability and antibacterial efficacy of FeNP nanoparticle conjugates. The nanoparticle conjugates were shaken in a bacterial suspension at 37°C for 4 hours, and OD_{600} was measured. The nanoparticle conjugates were readily collected at the side of the tube using a magnet and the supernatant was removed. To confirm the equimolar pairing of cobaltocenium moiety with anionic penicillin for the next cycle, a fresh batch of penicillin was added. The nanoparticles were washed multiple times with aqueous solution to remove any excess penicillin. Thus, obtained conjugates were re-dispersed in the bacterial solution and the procedure, mentioned earlier, was repeated. The enhanced inhibition efficiency of nanoparticle conjugates using the recycled nanoparticles against both Gram-positive and Gram-negative bacteria was retained even after five cycles (Figure 5 and Figure S5).

Cobaltocenium-containing iron oxide nanoparticles have dual mode of action: cationic cobaltocenium can disrupt cell membranes and the antibiotics target cell walls. We conducted a dose-dependent time-kill study to investigate how rapid the nanoparticle conjugates can kill bacteria using a colony formation assay. After incubating overnight with the nanoparticle conjugates, the solution was diluted and placed on an agar plate. The number of colony-forming units (CFU) was counted at various time up to 12 hours at the multiple of MIC concentration and expressed as $CFUmL^{-1}$. As shown in Figure 6,

nanoparticle conjugates started to act instantaneously, which can be seen by the significant reduction in bacteria concentration. With the concentration of just four times above the MIC, all bacteria (*S. aureus*) were completely killed in just 4 hours. When the concentration was increased to eight times of MIC, it took approximately one hour to kill all bacteria.

One of the main concerns on antimicrobial agents is that over time the bacteria evolve as a part of their adaptive response, and develop resistance, which cause an array of diseases ranging from minor infections to persistent and life-threatening infections. To evaluate the probability of that FeNP-penicillin conjugates might elicit resistance in bacteria, a resistance-selection study was conducted against both Gram-positive and Gram-negative bacteria using OD_{600} measurements. Cultures were subsampled and transferred 15 times to new media containing their respective antibiotic conjugates at MIC concentration. As shown in Figure 7, the OD_{600} values of the nanoparticle conjugates remained virtually constant even after 15 consecutive passages, indicating the nanoparticle conjugates did not induce drug resistance against both *S. aureus* and *E. coli.* In addition, the MIC values for *S. aureus* after 15 passages did not show any significant spikes ruling out any possibilities of resistance development (Figure S6 and Figure S7). The cobaltocenium-moiety has the capability to directly contact the bacterial cell wall causing disruption, which makes antibiotic resistance mechanism irrelevant for the conjugate system.

A typical bacterial cell is known to be in the micrometer range but the outer cell membranes consist of pores that are in the nanometer range. Thus, it enables the FeNP conjugates with diameters in the range of 30 nm to pass through the membrane to enter the cell causing the lysis of bacterial cells. As shown in Figure 8, the control bacterial cells are intact and have smooth surfaces. After treating with FeNP conjugates, outer cells membranes appeared to be disrupted with the entry of particles inside the cell and the bacterial cells seemed to have clumped together. This confers the particles can penetrate inside and cause lysis of bacterial cells.

Hemolysis is the lysis of red blood cells (RBC) and is commonly characterized as a side effect of cationic polymers. Therefore, a hemolytic assay was conducted to evaluate whether FeNP particles could lead to hemolysis of RBCs. We found that even at a concentration as high as 500 μg/mL, extremely low percentages of cells (< 5%) were lysed by FeNP compared to the negative control group, as shown in Figure S8. This implies that FeNP has negligible chances of creating hemolysis in the host cells.

Conclusions

In summary, we designed and synthesized highly efficient charged metallopolymer-grafted magnetic nanoparticles via surface-initiated RAFT polymerization. β-Lactam antibiotic penicillin-G was loaded onto the magnetic nanoparticles, based on electrostatic interaction between cationic cobaltocenium moiety and anionic antibiotic molecule. The resulting nanoparticle conjugates showed good bactericidal efficiencies against both Gram-positive and Gram-negative pathogenic strains, which facilitated the revitalization of the penicillin. These nanoparticles displayed a response to external magnetic fields and were easily recycled after antibacterial tests. The recycled nanoparticle conjugates retained aqueous dispersibility and high antibacterial efficacy. In addition, the nanoparticle conjugates killed

bacteria rapidly, and the susceptibility of both Gram-positive and Gram-negative strains to the nanoparticle conjugates remains almost unchanged even after 15 passages. The conjugates improved the bactericidal efficacy not only by rejuvenating antibiotics but also by providing an enhanced local concentration effect on the bacterial cells.

Experimental

Characterization

^{1}H (400 MHz), ^{13}C (100 MHz), and ^{19}F (376 MHz) NMR spectra were recorded on a Varian Mercury 400 NMR spectrometer with tetramethylsilane (TMS) as an internal reference. Mass spectrometry was conducted on a Waters Micromass Q-TOF mass spectrometer, and the ionization source was positive ion electrospray. UV–vis was carried out on a Shimadzu UV-2450 spectrophotometer with a 10.00 mm quartz cuvette and monochromatic light of various wavelengths over a range of 190–900 nm. A Hitachi 8000 transmission electron microscope (TEM) was applied to take images at an operating voltage of 150 kV. TEM samples were prepared by dropping solution on carbon-supported copper grids and then dried before observation. Dynamic light scattering (DLS) was operated on a Nano-ZS instrument, model ZEN 3600 (Malvern Instruments). Field-Emission Scanning Electron Microscopy (FE-SEM, Zeiss UltraPlus) was used to take images of bacterial cells after incubating overnight with test drugs. The samples were coated with gold using Denton Dest II Sputter Coater for 45 s and then observed by SEM.

Materials and Methods

2-Cobaltoceniumamidoethyl methacrylate hexafluorophosphate ($CoAEMAPF_6$) was synthesized according to our earlier reports[52, 56]. 2-Aminoethyl methacrylate hydrochloride (90%), *N*-(3-dimethylaminopropyl)-*N*′-ethylcarbodiimide hydrochloride (EDC-HCl, 98%), 4-(dimethylamino) pyridine and tetrabutylammonium chloride (TBACl) were purchased from Aldrich and used as received. Water was from Thermo Scientific Nanopure with ion conductivity at 18.2 MΩ. The following bacterial strains were purchased from ATCC: *Staphylococcus aureus* (*S. aureus*, ATCC-33591), *Bacillus cereus* (*B. cereus*, ATCC 11778), *Escherichia coli* (*E. coli*, ATCC-11775), *Klebsiella pneumoniae* (*K. pneumoniae*, ATCC-35596), *Proteus vulgaris* (*P. vulgaris* ATCC 33420). Nitrocefin was purchased from TOKU-E and used as received. Sodium salt of penicillin-G was purchased from VWR and used as received. 4-Cyanopentanoic acid dithiobenzoate (CPDB) was obtained from Strem Chemical Inc. Azobisisobutyronitrile (AIBN) was recrystallized from methanol before use. All other chemicals and reagents were from commercial sources and used as received.

Synthesis of iron oxide nanoparticles

The iron oxide nanoparticles were prepared by a co-precipitation method using a mixture of two salts ($FeCl_2$ and $FeCl_3$)[57]. Briefly, 0.01 mol $FeCl_2.4H_2O$ and 0.02 mol $FeCl_3.6H_2O$ were dissolved in 100 mL of deionized and deoxygenated water. Then, 0.08 mol of NaOH in 100 mL was added dropwise for 3 hours under nitrogen using a Soxhlet funnel while stirring. The precipitate was washed with water/ethanol repeatedly and dried in a desiccator for 24 hours. The RAFT agent was anchored in the nanoparticles following a reported

procedure[44]. In short, Iron oxide nanoparticles (0.5 g) was dispersed in dry THF and 3-aminopropyldimethylethoxysilane (0.32 mL, 1 mmol) was added. The mixture was refluxed in an oil bath for 6 h under nitrogen protection. After cooling to room temperature, the reaction was precipitated in 250 mL hexanes. The particles were precipitated three times and each time they were easily recovered by centrifugation. For the next part, 0.2 g, (0.4 mmol) of activated 4-cyano-4-(phenylcarbonylthioylthio)pentanoate (CPDB) was added dropwise to the dispersed solution of iron oxide nanoparticles in THF at room temperature. The solution was stirred overnight and precipitated in hexanes. The CPDB-anchored nanoparticles were recovered by centrifugation and dried in vacuum. The particles were then dispersed in THF and stored for later use.

Synthesis of cobaltocenium-containing iron oxide nanoparticles

$CoAEMAPF_6$ (200 mg, 0.41 mmol), CPDB-coated iron oxide nanoparticles (245 mg, 1 mmol) and 0.4 mL dry dimethyformamide (DMF) were added to a 10 mL Schlenk tube. To ensure good dispersion of nanoparticles, the solution was sonicated for 5 minutes, and AIBN (0.2 mg, 1.23 μmol) was added. The resulting solution was degassed by purging nitrogen for 30 minutes and then placed in an oil bath of 90 °C until the desired conversion was met. The polymerization was quenched by opening to air and cooling with ice water. The reaction mixture was precipitated in cold dichloromethane three times and vacuum-dried. Ion-exchange of Cl^- was performed according to a previous report using tetrabutylammonium chloride salt (TBACl) [53]. A typical procedure was as follows:1 mL PF_6^- paired FeNP (30 mg/mL in acetonitrile) was slowly dropped into 5 mL TBACl solution (in acetonitrile) under vigorous stirring. After stirring for 5 minutes, the precipitated Cl^- paired FeNP was collected and washed by acetonitrile three times to remove PF_6^- anions and excess TBACl. The solid yellow FeNP-Cl was then vacuum-dried and collected.

Synthesis of FeNP-Penicillin bioconjugates

Cobaltocenium-containing iron oxide nanoparticles with Cl^- was initially dispersed in deionized water and solution of penicillin-G sodium salt was added slowly with molar ratios (penicillin salt to cobaltocenium moieties) in the range of 1.15 to 1.0. The solution was stirred for 2 h and then dialyzed against 3L deionized water for 9 hours. The solution in a dialysis bag was collected and freeze-dried. The FeNP-Pen conjugates were obtained as a yellow powder.

Growth of bacteria

The antibacterial activity of cobaltocenium-containing iron oxide nanoparticles was evaluated using standard disk-diffusion assay (ASTM: the Kirby Bauer diffusion test)[55]. Firstly, actively-growing cultures of each bacterial strain on Mannitol salt agar (MSA) were inoculated on Tryptic Soy Broth (TSB) agar plates. The bacterial growth culture (cell concentrations were 1.0×10^6 CFU/mL) 10 μL was diluted to 1 mL in TSB, and 100 μL of cell culture was spread on TSB agar plates to form a bacterial lawn covering the plate surface. Then a 6 mm filter disc was laid on the agar surface, to which the nanoparticle solution was added at a desired concentration. All plates were incubated overnight at 37°C. The development of a clear zone around the disk was indicative of the ability of antimicrobial drugs to kill bacteria.

Bacterial morphology by FE-SEM

The morphologies of different bacteria after incubation with nanoparticle conjugates were examined by field-emission scanning electron microscopy (FE-SEM). In summary, 20 μL of bacterial cell solution was grown on one glass slide in a six-well plate containing 2 mL TSB medium at 37 °C overnight. Cell suspensions were diluted to OD_{600} = 1.0. After adding calculated amount of test drugs to the 1 mL cell stock solution, it was left to incubate overnight at 37 °C. A cell suspension without added chemicals was used as the control. The samples were then fixed in cacodylate buffered with 2.5% glutaraldehyde solution (pH = 7.2) for 2–3 h at 4 °C and post-fixed with 1% osmium tetroxide at 4 °C for 1 h. Samples were dehydrated under critical point, then coated with gold using Denton Dest II Sputter Coater for 120s and observed by FE-SEM.

LIVE/DEAD bacterial viability assays

The five bacterial strains were inoculated and prepared by a similar procedure as mentioned above. 1 mL of active bacterial stock solution was introduced to 5 μg penicillin solutions. An untreated cell suspension was used as the control. Following overnight incubation at 37°C, 1 μL LIVE/DEAD BacLight (Bacterial Viability Kit; Invitrogen Inc.) was added to the incubation solution. After incubation for 15 minutes, cells were imaged using a Leica TCS SP5 Confocal Scanning Laser Microscope with 63× oil-immersion lens. Stained cells were excited at 488 nm with a Krypton-Argon laser. Bacteria cells having intact membranes display green fluorescence (Emission = 515 nm) and bacteria with disrupted membranes fluoresce red (Emission = 635 nm).

Drug Resistance Study

50 μL aqueous solution of FeNP-penicillin conjugates with one-half the MIC concentration were added to 96-well plates. Then, 150 μL bacterial TSB solution (OD_{600} = 1.00) were added to the wells. The bacterial TSB solution without conjugates was used as the control. The assay plate was incubated at 37°C until the bacteria were grown to an optical density of about 1.00 (OD_{600} = ~ 1.00) in control samples. All assays were carried out in duplicate in the same assay plate. The process was repeated every 20-22h for up to 15 passages.

Recycling of FeNP-Pen for antibacterial assays

5 μl bacterial suspensions were inoculated into 3 mL TSB solutions at 37 °C for incubation at 300 rpm overnight. Identical bacterial culture solutions were prepared in three different tubes. The first tube was used as the control without adding any test samples while the second tube was used to determine the activity of penicillin. 2 × MIC of nanoparticle conjugates was added to the third tube before incubation. Bacterial growth was measured at OD_{600}, and was compared with the control tube. The inhibition efficiency was calculated as follows: inhibition efficiency (%) = (Control OD_{600} - Sample OD_{600})/ Control OD_{600} × 100. The control OD_{600} was determined from the blank tube. Each test was conducted in duplicate. After incubating overnight, the tube was placed adjacent to a magnet stand at room temperature for 10 min. The nanoparticles were attracted to the wall of the tube via magnetic force. After removing the supernatant from the tube, the nanoparticles were washed, and penicillin was added to result in nanoparticle conjugates. Any remaining

penicillin was removed by washing with aqueous solution. The test was then repeated for total of 5 passages.

Time-kill Study

The kinetics of antibacterial activity of nanoparticle conjugate was investigated. In summary, various concentrations of the nanoparticle conjugate were incubated at a time interval of 1 h, 2 h, 4 h, 6 h, 8 h and 12 h. During each interval, 100 μL of the culture solution was taken and diluted to 10^6 times. The final diluted solution was spread on agar plates to incubate at 37°C overnight and the colonies were counted next day. The experiment was carried out in duplicate.

Hemolysis evaluation for cytotoxicity determination

Blood was collected from mice in heparinized tubes and diluted by mixing 800 μL blood with 1000 μL PBS. Nanoparticle samples were prepared in PBS at concentrations 10, 50, 100 and 500 μg/mL and added 60 μL of the diluted blood samples to 3 mL of the nanoparticle conjugates, PBS or 0.1% Triton-X100 in PBS. The samples were incubated for 1 h at 37°C followed by centrifugation for 10 minutes at 1500 rpm. Supernatants were collected and OD was measured at 545 nm to calculate Hemolysis rate by using the formulae, HR=(AS-AN)/(AP-AN) where AS, AN and AP are OD values of the supernatants from test samples, negative control (PBS) and positive control (0.1% Triton-X100) respectively.

Supplementary Material

Refer to Web version on PubMed Central for supplementary material.

Acknowledgments

Research reported in this publication was supported in part by the National Institutes of Health Award #R01AI120987 and the National Science Foundation Award # OIA-1655740.

References

1Antibiotics Resistance Threats in the United States Center for Disease Control; 2013https://www.cdc.gov/drugresistance/threat-report-2013/pdf/ar-threats-2013-508.pdf

2Levy SB, Marshall B. Antibacterial resistance worldwide: causes, challenges and responses. Nat Med. 2004; 10:S122. [PubMed: 15577930]

3Ilker MF, Nüsslein K, Tew GN, Coughlin EB. Tuning the Hemolytic and Antibacterial Activities of Amphiphilic Polynorbornene Derivatives. J Am Chem Soc. 2004; 126:15870–5. [PubMed: 15571411]

4Kenawy ER, Worley SD, Broughton R. The Chemistry and Applications of Antimicrobial Polymers: A State-of-the-Art Review. Biomacromolecules. 2007; 8:1359–84. [PubMed: 17425365]

5Sambhy V, Peterson BR, Sen A. Antibacterial and Hemolytic Activities of Pyridinium Polymers as a Function of the Spatial Relationship between the Positive Charge and the Pendant Alkyl Tail. Angew Chem Int Ed. 2008; 47:1250–4.

6Tew GN, Liu D, Chen B, Doerksen RJ, Kaplan J, Carroll PJ, et al. *De novo* design of biomimetic antimicrobial polymers. Proc Natl Acad Sci USA. 2002; 99:5110–4. [PubMed: 11959961]

7Engler AC, Wiradharma N, Ong ZY, Coady DJ, Hedrick JL, Yang YY. Emerging trends in macromolecular antimicrobials to fight multi-drug-resistant infections. Nano Today. 2012; 7:201–22.

8Takahashi H, Caputo GA, Vemparala S, Kuroda K. Synthetic Random Copolymers as a Molecular Platform To Mimic Host-Defense Antimicrobial Peptides. Bioconj Chem. 2017; 28:1340–50.

9Mizutani M, Palermo EF, Thoma LM, Satoh K, Kamigaito M, Kuroda K. Design and Synthesis of Self-Degradable Antibacterial Polymers by Simultaneous Chain- and Step-Growth Radical Copolymerization. Biomacromolecules. 2012; 13:1554–63. [PubMed: 22497522]

10Ganewatta MS, Tang C. Controlling macromolecular structures towards effective antimicrobial polymers. Polymer. 2015; 63:A1–A29.

11Sang P, Shi Y, Teng P, Cao A, Xu H, Li Q, et al. Antimicrobial AApeptides. Curr Top Med Chem. 2017; 17:1266–79. [PubMed: 27758686]

12Pelgrift RY, Friedman AJ. Nanotechnology as a therapeutic tool to combat microbial resistance. Adv Drug Del Rev. 2013; 65:1803–15.

13Guo S, Zhang S, Sun S. Tuning Nanoparticle Catalysis for the Oxygen Reduction Reaction. Angew Chem Int Ed. 2013; 52:8526–44.

14Govan J, Gun'ko Y. Recent Advances in the Application of Magnetic Nanoparticles as a Support for Homogeneous Catalysts. Nanomaterials. 2014; 4:222. [PubMed: 28344220]

15Wu L, Mendoza-Garcia A, Li Q, Sun S. Organic Phase Syntheses of Magnetic Nanoparticles and Their Applications. Chem Rev. 2016; 116:10473–512. [PubMed: 27355413]

16Weller D, Mosendz O, Parker G, Pisana S, Santos TS. L10 FePtX–Y media for heat-assisted magnetic recording. physica status solidi (a). 2013; 210:1245–60.

17Takafuji M, Ide S, Ihara H, Xu Z. Preparation of Poly(1-vinylimidazole)-Grafted Magnetic Nanoparticles and Their Application for Removal of Metal Ions. Chem Mater. 2004; 16:1977–83.

18Li Z, Wei L, Gao MY, Lei H. One-Pot Reaction to Synthesize Biocompatible Magnetite Nanoparticles. Adv Mater. 2005; 17:1001–5.

19Ulbrich K, Holá K, Šubr V, Bakandritsos A, Tuček J, Zbořil R. Targeted Drug Delivery with Polymers and Magnetic Nanoparticles: Covalent and Noncovalent Approaches, Release Control, and Clinical Studies. Chem Rev. 2016; 116:5338–431. [PubMed: 27109701]

20Gupta AK, Gupta M. Synthesis and surface engineering of iron oxide nanoparticles for biomedical applications. Biomaterials. 2005; 26:3995–4021. [PubMed: 15626447]

21Dong H, Huang J, Koepsel RR, Ye P, Russell AJ, Matyjaszewski K. Recyclable Antibacterial Magnetic Nanoparticles Grafted with Quaternized Poly(2-(dimethylamino)ethyl methacrylate) Brushes. Biomacromolecules. 2011; 12:1305–11. [PubMed: 21384911]

22Wang L, Cole M, Li J, Zheng Y, Chen YP, Miller KP, et al. Polymer grafted recyclable magnetic nanoparticles. Polym Chem. 2015; 6:248–55.

23Xu C, Sun S. Monodisperse magnetic nanoparticles for biomedical applications. Polym Int. 2007; 56:821–6.

24Lu AH, Salabas EL, Schüth F. Magnetic Nanoparticles: Synthesis, Protection, Functionalization, and Application. Angew Chem Int Ed. 2007; 46:1222–44.

25Balazs AC, Emrick T, Russell TP. Nanoparticle Polymer Composites: Where Two Small Worlds Meet. Science. 2006; 314:1107–10. [PubMed: 17110567]

26Kohut A, Ranjan S, Voronov A, Peukert W, Tokarev V, Bednarska O, et al. Design of a New Invertible Polymer Coating on a Solid Surface and Its Effect on Dispersion Colloidal Stability. Langmuir. 2006; 22:6498–506. [PubMed: 16830990]

27Hill LJ, Pinna N, Char K, Pyun J. Colloidal polymers from inorganic nanoparticle monomers. Prog Polym Sci. 2015; 40:85–120.

28Kango S, Kalia S, Celli A, Njuguna J, Habibi Y, Kumar R. Surface modification of inorganic nanoparticles for development of organic–inorganic nanocomposites—A review. Prog Polym Sci. 2013; 38:1232–61.

29von Werne T, Patten TE. Atom Transfer Radical Polymerization from Nanoparticles: A Tool for the Preparation of Well-Defined Hybrid Nanostructures and for Understanding the Chemistry of

Controlled/“Living” Radical Polymerizations from Surfaces. J Am Chem Soc. 2001; 123:7497–505. [PubMed: 11480969]

30D'Costa VM, King CE, Kalan L, Morar M, Sung WWL, Schwarz C, et al. Antibiotic resistance is ancient. Nature. 2011; 477:457. [PubMed: 21881561]

31Zhang J, Chen YP, Miller KP, Ganewatta MS, Bam M, Yan Y, et al. Antimicrobial Metallopolymers and Their Bioconjugates with Conventional Antibiotics against Multidrug-Resistant Bacteria. J Am Chem Soc. 2014; 136:4873–6. [PubMed: 24628053]

32Yang P, Bam M, Pageni P, Zhu T, Chen YP, Nagarkatti M, et al. Trio Act of Boronolectin with Antibiotic-Metal Complexed Macromolecules toward Broad-Spectrum Antimicrobial Efficacy. ACS Infectious Diseases. 2017; 3:845–53. [PubMed: 28976179]

33Pageni P, Yang P, Chen YP, Huang Y, Bam M, Zhu T, et al. Charged Metallopolymer-Grafted Silica Nanoparticles for Antimicrobial Applications. Biomacromolecules. 2018; 19:417–25. [PubMed: 29384661]

34Ren L, Hardy CG, Tang C. Synthesis and Solution Self-Assembly of Side-Chain Cobaltocenium-Containing Block Copolymers. J Am Chem Soc. 2010; 132:8874–5. [PubMed: 20540580]

35Yang P, Pageni P, Kabir MP, Zhu T, Tang C. Metallocene-Containing Homopolymers and Heterobimetallic Block Copolymers via Photoinduced RAFT Polymerization. ACS Macro Lett. 2016; 5:1293–300. [PubMed: 29276651]

36Yan Y, Pageni P, Kabir MP, Tang C. Metallocenium Chemistry and Its Emerging Impact on Synthetic Macromolecular Chemistry. Synlett. 2016; 27:984–1005.

37Yan Y, Zhang J, Wilbon P, Qiao Y, Tang C. Ring-Opening Metathesis Polymerization of 18-e Cobalt(I)-Containing Norbornene and Application as Heterogeneous Macromolecular Catalyst in Atom Transfer Radical Polymerization. Macromol Rapid Commun. 2014; 35:1840–5. [PubMed: 25250694]

38Zhang J, Yan Y, Chen J, Chance WM, Hayat J, Gai Z, et al. Nanostructured Metal/Carbon Composites from Heterobimetallic Block Copolymers with Controlled Magnetic Properties. Chem Mater. 2014; 26:3185–90.

39Zhu T, Xu S, Rahman A, Dogdibegovic E, Yang P, Pageni P, et al. Cationic Metallo-Polyelectrolytes for Robust Alkaline Anion-Exchange Membranes. Angew Chem Int Ed. 2018; doi: 10.1002/anie.201712387

40Rapakousiou A, Wang Y, Belin C, Pinaud N, Ruiz J, Astruc D. ‘Click’ Synthesis and Redox Properties of Triazolyl Cobalticinium Dendrimers. Inorg Chem. 2013; 52:6685–93. [PubMed: 23692324]

41Mayer UFJ, Gilroy JB, O'Hare D, Manners I. Ring-Opening Polymerization of 19-Electron [2]Cobaltocenophanes: A Route to High-Molecular-Weight, Water-Soluble Polycobaltocenium Polyelectrolytes. J Am Chem Soc. 2009; 131:10382–3. [PubMed: 19586050]

42Yan Y, Zhang J, Ren L, Tang C. Metal-containing and related polymers for biomedical applications. Chem Soc Rev. 2016; 45:5232–63. [PubMed: 26910408]

43Petcharoen K, Sirivat A. Synthesis and characterization of magnetite nanoparticles via the chemical co-precipitation method. Materials Science and Engineering: B. 2012; 177:421–7.

44Li C, Han J, Ryu CY, Benicewicz BC. A Versatile Method To Prepare RAFT Agent Anchored Substrates and the Preparation of PMMA Grafted Nanoparticles. Macromolecules. 2006; 39:3175–83.

45Hill MR, Carmean RN, Sumerlin BS. Expanding the Scope of RAFT Polymerization: Recent Advances and New Horizons. Macromolecules. 2015; 48:5459–69.

46Roy D, Guthrie JT, Perrier S. Graft Polymerization: Grafting Poly(styrene) from Cellulose via Reversible Addition-Fragmentation Chain Transfer (RAFT) Polymerization. Macromolecules. 2005; 38:10363–72.

47Lin EW, Maynard HD. Grafting from Small Interfering Ribonucleic Acid (siRNA) as an Alternative Synthesis Route to siRNA–Polymer Conjugates. Macromolecules. 2015; 48:5640–7.

48Cobo I, Li M, Sumerlin BS, Perrier S. Smart hybrid materials by conjugation of responsive polymers to biomacromolecules. Nat Mater. 2014; 14:143. [PubMed: 25401924]

49Kumar SK, Jouault N, Benicewicz B, Neely T. Nanocomposites with Polymer Grafted Nanoparticles. Macromolecules. 2013; 46:3199–214.

50Boyer C, Bulmus V, Davis TP, Ladmiral V, Liu J, Perrier S. Bioapplications of RAFT Polymerization. Chem Rev. 2009; 109:5402–36. [PubMed: 19764725]

51Moad G, Chong YK, Postma A, Rizzardo E, Thang SH. Advances in RAFT polymerization: the synthesis of polymers with defined end-groups. Polymer. 2005; 46:8458–68.

52Pageni P, Kabir MP, Yang P, Tang C. Binding of Cobaltocenium-Containing Polyelectrolytes with Anionic Probes. Journal of Inorganic and Organometallic Polymers and Materials. 2017; 27:1100–9. [PubMed: 29097986]

53Zhang J, Yan Y, Chance MW, Chen J, Hayat J, Ma S, et al. Charged Metallopolymers as Universal Precursors for Versatile Cobalt Materials. Angew Chem Int Ed. 2013; 52:13387–91.

54Bauer AW, Kirby WM, Sherris JC, Turck M. Antibiotic susceptibility testing by a standardized single disk method. Am J Clin Pathol. 1966; 45:493–6. [PubMed: 5325707]

55Wiegand I, Hilpert K, Hancock REW. Agar and broth dilution methods to determine the minimal inhibitory concentration (MIC) of antimicrobial substances. Nat Protoc. 2008; 3:163. [PubMed: 18274517]

56Zhang J, Yan J, Pageni P, Yan Y, Wirth A, Chen YP, et al. Anion-Responsive Metallopolymer Hydrogels for Healthcare Applications. Sci Rep. 2015; 5:11914. [PubMed: 26202475]

57Mascolo M, Pei Y, Ring T. Room Temperature Co-Precipitation Synthesis of Magnetite Nanoparticles in a Large pH Window with Different Bases. Materials. 2013; 6:5549. [PubMed: 28788408]

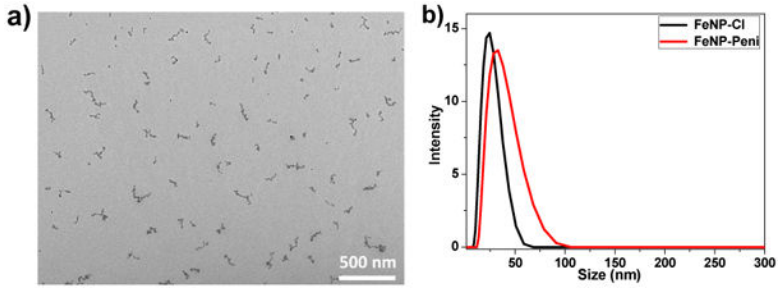

Figure 1.

a) TEM image of FeNP-Cl nanoparticles; and b) Dynamic Light Scattering (DLS) measurements showing sizes of nanoparticles.

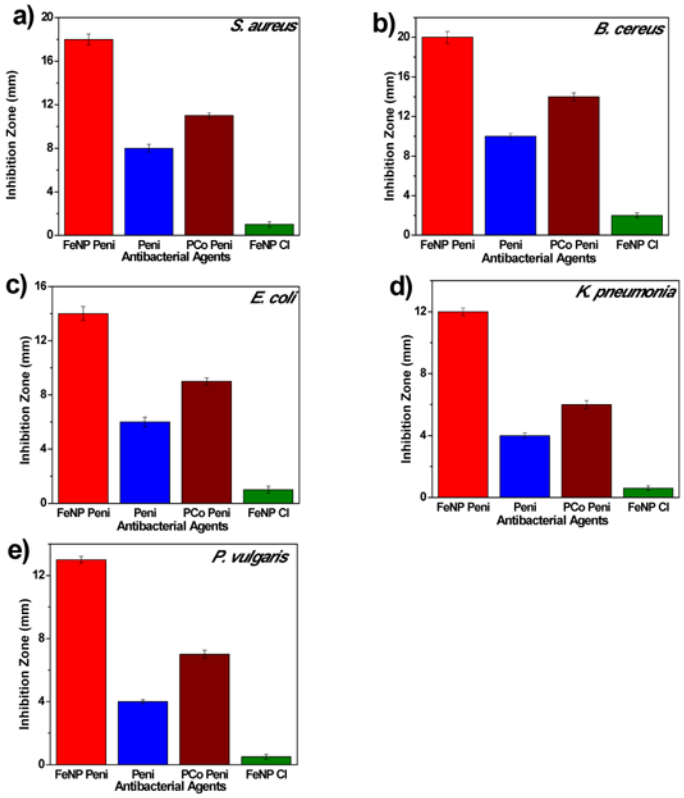

Figure 2.

Inhibition zones of different agents against various strains of bacteria at an equivalent of 7 μg penicillin-G/disk using disk-diffusion assays: a) *S. aureus*; b) *B. cereus* C) *E. coli;* d) *K. pneumoniae*; e) *P. vulgaris.*

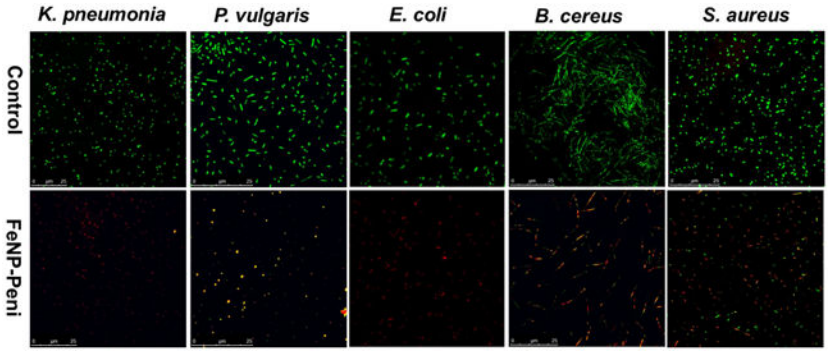

Figure 3.

Confocal scanning laser microscopy (CSLM) images of bacteria exposed to a concentration equivalent of penicillin 7 μg/mL: control *vs.* FeNP-penicillin conjugates. Bacterial cells, *K. pneumonia, P. vulgaris, E. coli, B. cereus and S. aureus,* were stained using BacLight Live/Dead stain, where green indicates live cells, and red indicates dead cells). The bacterial solution without FeNP was used as the control.

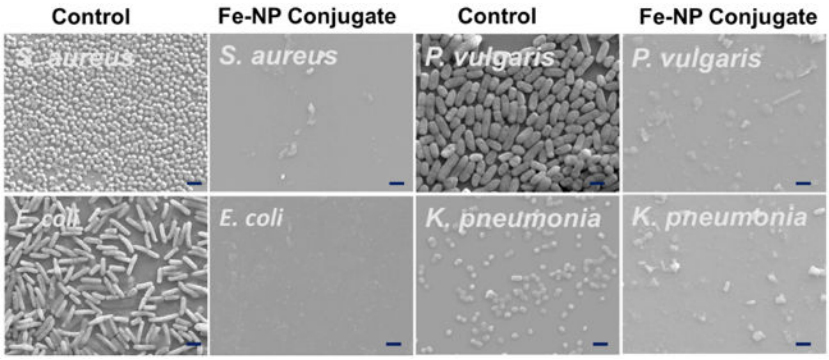

Figure 4.

Scanning electron microscopy (SEM) images of control and FeNP-penicillin conjugates with a concentration of penicillin at 7 μg/mL against various Gram-positive and Gram-negative bacteria. Bacterial solutions without FeNP were used as the control. All scale bars are 2.0 μm.

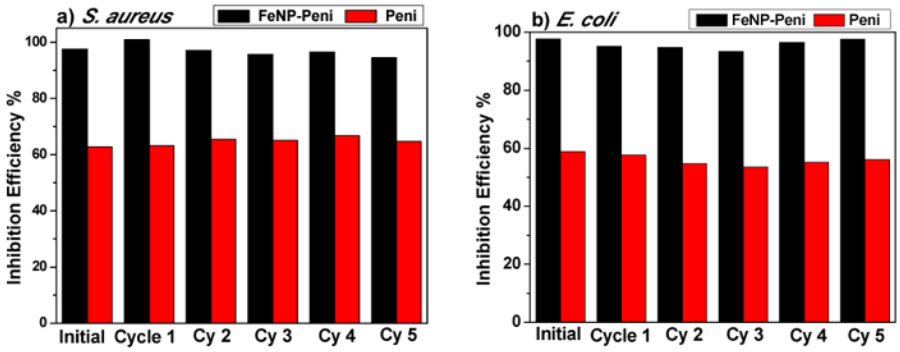

Figure 5.

Inhibition activities of recyclable magnetic cobaltocenium-containing FeNP conjugates against Gram-positive (*S. aureus*) and Gram-negative bacteria (*E. coli*).

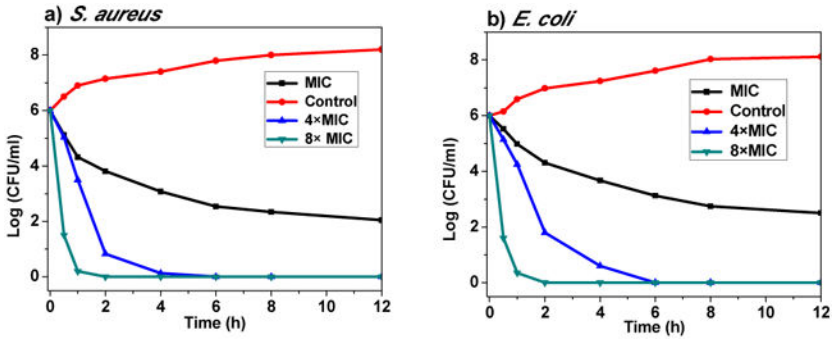

Figure 6.

Time-kill curves of FeNP-conjugates against *S. aureus* and *E. coli*. Bactericidal activities were monitored for first 12 hours. The concentrations used were MIC, 4×MIC, and 8×MIC, respectively.

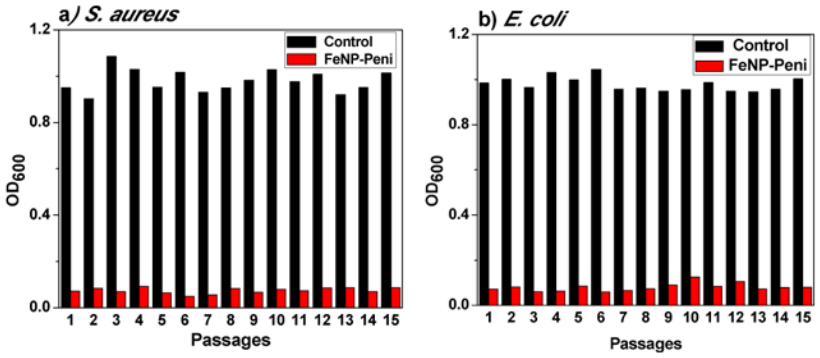

Figure 7.
Drug resistance study of FeNP-penicillin conjugates against *S. aureus* and *E. coli*.

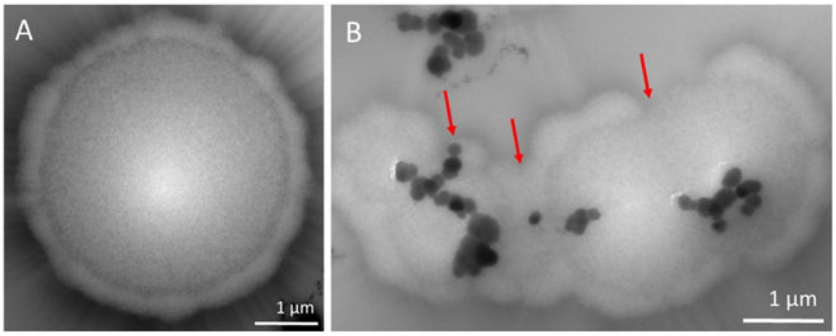

Figure 8.

TEM images of *S. aureus* after incubating with (A) Control; and (B) FeNP-conjugates, with the concentration of penicillin at 7 μg/mL.

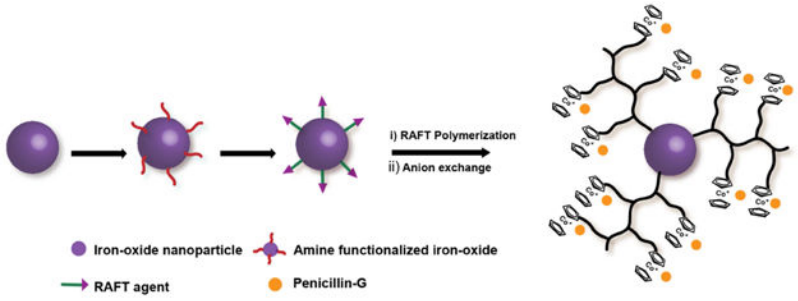

Scheme 1.

Synthesis of cobaltocenium-containing silica nanoparticles by surface-initiated RAFT polymerization.

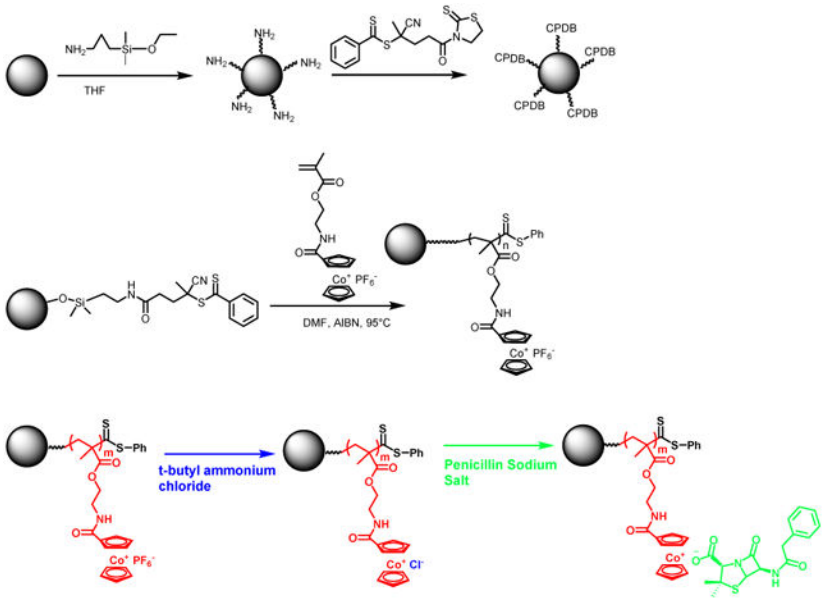

Scheme 2.
Modification of iron oxide nanoparticles using cobaltocenium-containing polymer by RAFT.

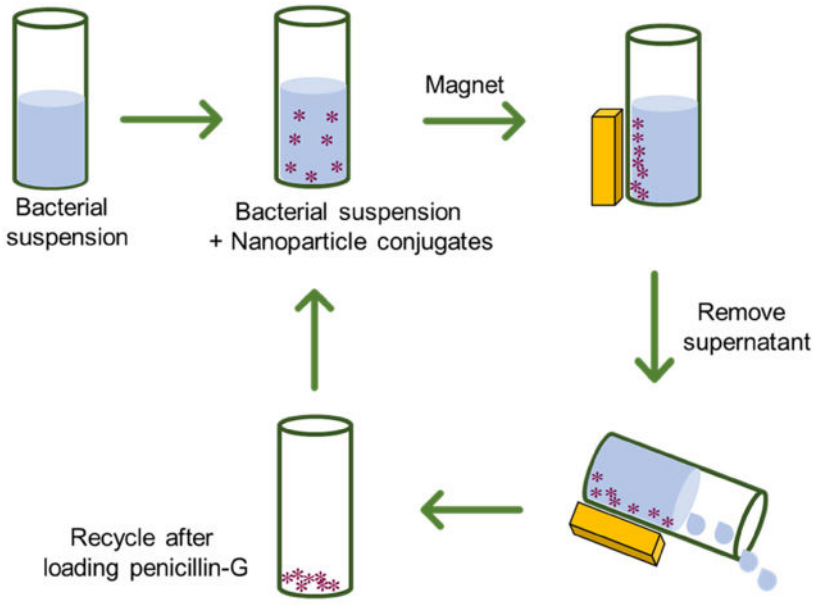

Scheme 3.

Schematic illustration of recycling cobaltocenium-containing magnetic nanoparticles for antibacterial application.

Table 1

Minimum inhibitory concentrations (MICs) of different agents against five strains of bacteria.

Entry	Minimum Inhibitory Concentration (MIC μg/mL)				
	S. aureus	B. cereus	E. coli	P. vulgaris	K. pneumonia
FeCo-Pen	3.4	2.7	5.6	6.5	7.6
Penicillin	13.5	10.9	22.3	17.5	26.7